J. Appl. Cryst. (1999). **32**, 281–289

Phenomenological model of anisotropic peak broadening in powder diffraction

Peter W. Stephens

National Synchrotron Light Source, Brookhaven National Laboratory, Upton, NY 11973, USA, and Department of Physics and Astronomy, State University of New York, Stony Brook, New York 11974-3800, USA.
E-mail: pstephens@sunnysb.edu

(*Received 9 December 1997; accepted 29 September 1998*)

Abstract

Anisotropic line-shape broadening (peak width which is not a smooth function of *d*-spacing) is frequently observed in powder diffraction patterns, and can be a source of considerable difficulty for whole-pattern fitting or Rietveld analysis. A model of the multi-dimensional distribution of lattice metrics within a powder sample is developed, leading naturally to a few parameters which can be varied to achieve optimal line-shape fits. Conditions on these parameters are derived for all crystal systems, and the method is illustrated with two examples: sodium *p*-hydroxybenzoate and rubidium fulleride.

1. Introduction

The development of high-resolution powder diffraction, especially at synchrotron radiation and pulsed neutron sources, both allows and requires an accurate description of the diffraction line shape. The original Rietveld (1969) formulation and many of its successors (*e.g.* Thompson, Cox & Hastings, 1987) treat the diffraction line width as a smooth function of *d*-spacing or diffraction angle 2θ, whereas, for many samples of interest, peaks nearby in 2θ have vastly different widths. We consider here the case of a distribution of strain, in which the diffraction peak width increases in proportion to the diffraction order. Diffraction widths which are not a smooth function of *d* might also arise from anisotropic sample size broadening or from a particular pattern of defects (*e.g.* stacking faults), but such cases are not covered in the present work. Readers interested in the approaches which have been used to treat anisotropic strain (and size) broadening are referred to the review by Le Bail (1992).

The simplest case of strain broadening is isotropic or uniform strain, which, for a fixed-wavelength diffraction experiment, leads to a diffraction-peak full width at half-maximum (FWHM) in 2θ proportional to $\tan\theta$, *i.e.* $\Gamma_{2\theta} = X\tan\theta$. In many cases, this does not provide an adequate description of the systematic variation of line shape. A Williamson–Hall plot (scatter plot of $\Gamma_{2\theta}/\cos\theta$ *versus* $\sin\theta$) is helpful in distinguishing the cause of anisotropic broadening of diffraction peaks.

One of the empirical approaches to anisotropic strain is found to be useful if there is one particular direction of maximum strain within the crystal, so that one may take $\Gamma_{2\theta} = (X + X_e\cos\Phi)\tan\theta$, where Φ is the angle between the diffraction peak under consideration and the strain axis. This provides an improved fit in certain cases, but is clearly inadequate for many applications. The method has been generalized by several authors to a strain distribution which broadens peaks as an ellipsoid in reciprocal space similar to the formalism used for anisotropic temperature factors. While the details differ among these treatments, they share the common feature that the width of the diffraction peak is expressed in terms of the six components of a symmetric tensor of the Miller indices. For example, this expansion has been applied to the parameters *U*, *V* and *W* of Caglioti *et al.* (1958) by Le Bail & Jouanneaux (1997), such that

$$U_{hkl} = d_{hkl}^2(A_{11}h^2 + \cdots A_{23}kl)$$

and likewise for *V* and *W*, and to the width of the neutron time-of-flight peak by David & Jorgensen (1995),

$$\Gamma_{\rm TOF} = d_{hkl}^2(A_{11}h^2 + \cdots A_{23}kl)^{1/2}.$$

as well as by Von Dreele & Line (1997),

$$\Gamma_{\rm TOF} = d_{hkl}^3(A_{11}h^2 + \cdots A_{23}kl).$$

These methods have been successful in producing improved line-shape fits, even though no theoretical justification or microscopic model has been given.

A different approach, equally empirical, has been developed by Cox (1994), originally for the cubic crystal system, and subsequently generalized. (The ellipsoidal broadening model cannot be applied to cubic crystals because the only ellipsoid with cubic symmetry is a sphere.) Cox has developed a formalism in which the width is separated into the product of a 2θ term and a function of the direction of the diffraction peak relative to the lattice, $\hat{Q}$, *e.g.* $\Gamma_{2\theta} = f(2\theta)g(\hat{Q})$. This may be cast in a useful form for line-shape fitting if $g(\hat{Q})$ can be described with a limited number of parameters, *e.g.* spherical harmonics adapted to the crystal symmetry. Cox and others have used this approach to obtain a

significant improvement in the quality of fits for cubic K_3C_{60} and Rb_3C_{60} (Cox, 1994; Fischer *et al.*, 1995).

A completely different viewpoint is to consider the distribution of lattice metric parameters within a sample. Each crystallite is regarded as having its own lattice parameters, with a multi-dimensional distribution throughout the powder sample. The width of each reflection can be expressed in terms of moments of this distribution, which leads naturally to parameters that can be varied to achieve optimal line-shape fits. This approach has been described previously (Thompson, Reilly & Hastings, 1987; Rodríguez-Carvajal *et al.*, 1991; Rodríguez-Carvajal, 1997), but there are certain deficiencies in the published work that must be remedied in order for it to be generally applicable. Specifically, it has been restricted to the Gaussian component of the line shape and the formulations do not obey the lattice symmetry (Thompson, Reilly & Hastings, 1987), or are not as general as required (Rodríguez-Carvajal, 1997). This paper presents a model of anisotropic peak broadening through correlations between metric parameters, compares the model with previous work, and illustrates it with two examples.

2. Model of anisotropic broadening

The spacing d between lattice planes for any given reflection defined by the Miller indices hkl is given by

$$1/d^2 = M_{hkl} = Ah^2 + Bk^2 + Cl^2 + Dkl + Ehl + Fhk \tag{1}$$

where $\{A, \ldots, F\}$ are metric parameters of the reciprocal lattice. We consider strain broadening as a manifestation of the distribution of the parameters, so that each individual grain is imagined to have its own set of $\{A, \ldots, F\}$, differing from $\{\langle A\rangle, \ldots, \langle F\rangle\}$. Note that the local values of $\{A, \ldots, F\}$ need not respect the symmetry of the sample as a whole. For example, in a cubic material, $\langle A\rangle = \langle B\rangle = \langle C\rangle$ and $\langle D\rangle = \langle E\rangle = \langle F\rangle = 0$, but an individual grain may deviate from these conditions. Hence, even though the crystalline symmetry may require that the mean of some of the parameters be zero, there may be a distribution about zero for a sample incorporating random strains.

For notational convenience, we relabel the parameters $\{A, \ldots, F\}$ as $\{\alpha_i: i = 1, \ldots, 6\}$. Assume for the moment that the α_i parameters have a Gaussian distribution characterized by a covariance matrix $C_{ij} = \langle(\alpha_i - \langle a_i\rangle)(\alpha_j - \langle\alpha_j\rangle)\rangle$, with $C_{ii} = \sigma^2(\alpha_i)$, the variance of α_i. M_{hkl} is linear in α_i, and so from elementary statistics (see, *e.g.* Mendenhall *et al.*, 1986), the variance of M_{hkl} is given by

$$\sigma^2(M_{hkl}) = \sum_{i,j} C_{ij} \frac{\partial M}{\partial \alpha_i} \frac{\partial M}{\partial \alpha_j}. \tag{2}$$

Note that $\partial M/\partial\alpha_1 = h^2$, $\partial M/\partial\alpha_6 = hk$, *etc.* Therefore, (2) can be rearranged as

$$\sigma^2(M_{hkl}) = \sum_{HKL} S_{HKL} h^H k^K l^L \tag{3}$$

with terms S_{HKL} defined for $H + K + L = 4$. In the most general (triclinic) case, there are 15 such independent parameters S_{HKL}, as opposed to the 21 elements of C_{ij}. This is due to a geometric redundancy of the C_{ij} in (2). For example, it is meaningless to distinguish a positive correlation of the magnitudes of the reciprocal lattice parameters a^* and b^* (appearing as C_{12}) from the variance of the angle γ^* between them (incorporated into C_{66}). Both produce contributions proportional to h^2k^2 in (2), and so C_{12} and C_{66} are not independent, whereas there is only one parameter in (3) proportional to h^2k^2, namely S_{220}.

Using the Bragg equation, $\sin\theta = \lambda/(2d) = \lambda M^{1/2}/2$, the anisotropic broadening contribution to the FWHM (in radians) of a diffraction line is given by

$$\Gamma_A = [\sigma^2(M_{hkl})]^{1/2} \tan\theta/M_{hkl}. \tag{4}$$

[Here, the factor of $(8\ln 2)^{1/2}$ between the r.m.s. and the FWHM of a Gaussian has been incorporated into the definition of S_{HKL}.] A similar result for the peak width as a function of $\sigma^2(M_{hkl})$ may be derived for time-of-flight neutron diffraction.

Powder diffraction line shapes are generally not Gaussian. One widely used line shape for Rietveld analysis of diffraction profiles consists of a convolution of Gaussian and Lorentzian line shapes, commonly known as the Voigt line shape. Taking the Gaussian and Lorentzian line-shape functions with FWHM Γ, normalized to unit integrated intensity,

$$G_\Gamma(x) = [(4\ln 2/\pi)^{1/2}/\Gamma]\exp -(4\ln 2x^2/\Gamma^2)$$
$$L_\Gamma(x) = (\Gamma/2\pi)/[(\Gamma/2)^2 + x^2],$$

the Voigt line shape of a peak centered at $2\theta_0$ is defined as

$$V_{\Gamma_G,\Gamma_L}(2\theta - 2\theta_0) = \int \mathrm{d}2\theta' G_{\Gamma_G}(2\theta - 2\theta') \times L_{\Gamma_L}(2\theta' - 2\theta_0).$$

Following Thompson, Cox & Hastings (1987), the Gaussian and Lorentzian widths are often taken to depend on the scattering angle 2θ as

$$\Gamma_G = (U\tan^2\theta + V\tan\theta + W)^{1/2} \tag{5a}$$

and

$$\Gamma_L = X\tan\theta + Y/\cos\theta \tag{5b}$$

respectively, and the parameters $U, \ldots, Y$ are adjusted to give the best fit to the line shape.

The generalization of equations (3) and (4) to incorporate a Lorentzian term in the line shape is difficult, because the Lorentzian does not have a second moment,

Table 1. *Restrictions on anisotropic strain parameters for the seven crystal systems*

Those S_{HKL} not listed in the last column must be zero.

Crystal system	Restrictions on metric parameters	Anisotropic strain parameters
Cubic	$A = B = C, D = E = F = 0$	$S_{400} = S_{040} = S_{004}$, $S_{220} = S_{202} = S_{022}$
Tetragonal	$A = B, D = E = F = 0$	$S_{400} = S_{040}$, $S_{202} = S_{022}$, S_{004}, S_{220}
Orthorhombic	$D = E = F = 0$	S_{400}, S_{040}, S_{004}, S_{220}, S_{202}, S_{022}
Monoclinic	$D = F = 0$	S_{400}, S_{301}, S_{220}, S_{202}, S_{121}, S_{103}, S_{040}, S_{022}, S_{004}
Trigonal (*R*3 *etc.*)	$A = B = C, D = E = F$	Rhombohedral indices: $S_{400} = S_{040} = S_{004}$, $S_{220} = S_{202} = S_{022}$, $S_{211} = S_{121} = S_{112}$, $S_{310} = S_{130} = S_{301} = S_{103} = S_{031} = S_{013}$ Hexagonal indices: $S_{400} = S_{040} = S_{310}/2 = S_{130}/2 = S_{220}/3$, $S_{202} = S_{022} = S_{112}$, S_{004}, $S_{301}/2 = -S_{031}/2 = S_{211}/3 = -S_{121}/3$
Hexagonal, trigonal (*P*3 *etc.*)	$A = B = F, D = E = 0$	$S_{400} = S_{040} = S_{310}/2 = S_{130}/2 = S_{220}/3$, $S_{202} = S_{022} = S_{112}$, S_{004}
Triclinic		All 15 S_{HKL} allowed

and thus the argument leading to (2) is not valid. In particular, even though the convolution of two Lorentzians is a Lorentzian (of the sum of the original widths), there is no generalization of a Lorentzian line shape to higher dimensions such that any projection yields a Lorentzian. Nevertheless, it is important to be able to incorporate a Lorentzian line shape into this formalism; consequently, we assume, without further mathematical justification, that equations (3) and (4) can be interpreted to give the FWHM of a Lorentzian anisotropic broadening term. In order to have a method for interpolation between Gaussian and Lorentzian, we introduce a parameter ζ and consider an anisotropically broadened Voigt line shape, $V_{(1-\zeta)\Gamma_A,\zeta\Gamma_A}(2\theta - 2\theta_0)$, with Gaussian and Lorentzian widths $(1-\zeta)\Gamma_A$ and $\zeta\Gamma_A$, respectively. Note that the FWHM of this function differs from Γ_A if ζ differs from 0 or 1.

Making use of the familiar results for the convolution of two Gaussian or two Lorentzian line shapes, the widths are taken to be

$$\Gamma_G = [U\tan^2\theta + V\tan\theta + W + (1-\zeta)^2\Gamma_A^2(hkl)]^{1/2}$$
$$\Gamma_L = X\tan\theta + Y/\cos\theta + \zeta\Gamma_A(hkl). \tag{6}$$

Often, X and U are interpreted as incorporating strain contributions, and so they may duplicate the action of the S_{HKL} parameters introduced here. In actual use, they may be set by fitting some reference standard. They also allow the possibility of parameterizing different line shapes for broad and sharp peaks, should such a case arise. The shape of reflections for which $\Gamma_A(hkl)$ is small will be governed by $U, \ldots, W$, whereas the shape of peaks having a large $\Gamma_A(hkl)$ is controlled by ζ.

There are certain restrictions on the allowed anisotropic broadening terms based on the crystal system. For example, in a cubic crystal, reflections (hkl), (khl), (lhk), $(\bar{h}kl)$, *etc.* all coincide, and should therefore have the same width. This leads to the restrictions on strain parameters listed in Table 1. All of these restrictions are fairly obvious by inspection, except perhaps for those of the hexagonal system. In that case, reflections (hkl), $(hk\bar{l})$, $(h+k, \bar{k}, l)$, *etc.* are equivalent, implying that h and k can enter only in the combination $h^2 + k^2 + hk$. The only possible terms are therefore proportional to $(h^2 + k^2 + hk)^2$, $(h^2 + k^2 + hk)l^2$, and l^4.

The trigonal (rhombohedral) Bravais lattice is generated by three primitive vectors of equal length, separated by equal angles. However, the diffraction patterns of trigonal crystals are frequently indexed by hexagonal axes. The fact that rhombohedral reciprocal lattices have four independent anisotropic strain parameters while hexagonal diffraction patterns admit only three may seem confusing. For example, in the present formalism, the strain-broadened widths of rhombohedral peaks in the four directions (100), (110), $(1\bar{1}0)$ and (111) are linearly independent; these translate into hexagonal indices (101), (012), $(2\bar{1}0)$ and (003), of which only three can be adjusted independently. The resolution is that when hexagonal indices are used for the seven rhombohedral space groups $R3$, $R\bar{3}$, $R32$, $R3m$, $R\bar{3}m$, $R3c$ and $R\bar{3}c$, only peaks with $-h + k + l \equiv 0 \bmod 3$ are observed. The spurious sixfold axis can be removed in these cases where it is desired to use hexagonal indices by introducing a fourth strain parameter as

a coefficient to $[3h^3 - 3k^3 + (k-h)^3]l$, a combination of indices which has $\bar{3}$ symmetry.

3. Examples

This section illustrates the formalism developed above by application to two systems: monoclinic sodium *p*-hydroxybenzoate ($NaO_2C_7H_4OH$) and cubic Rb_3C_{60}. The model of anisotropic broadening for Rietveld and Le Bail fitting of fixed-wavelength data described above has been realized in a program *TPROFPV*, adapted from the program *PROFPV*, which was adapted by D. E. Cox, B. H. Toby, P. Zolliker & J. A. Hriljac from the original Rietveld (1969) program.

3.1. *Sodium p-hydroxybenzoate*

The crystal structure of NaO_2C-C_6H_4-*p*-OH was unknown before this work; a preliminary report has been given by Dinnebier *et al.* (1995). However, due to severe anisotropic broadening, conventional Rietveld refinements could not produce a sufficiently low *R* factor to give confidence that the details of the structure were correct. Indeed, the data set provided the main motivation for the present work on anisotropic line-shape broadening.

The synthesis and structure of this material will be described in another publication. The air-sensitive sample was sealed in a thin-walled glass capillary and a diffraction data set was recorded at beamline X3B1 of the National Synchrotron Light Source. X-rays of wavelength 1.1475 Å were selected by a double-crystal Si(111) monochromator, and the diffracted radiation analyzed by a Ge(111) crystal before a scintillation detector. X-ray counts were normalized to the signal from an ionization chamber to correct for the decay of current in the storage ring. The data were collected in steps of 0.005° of 2θ from 3 to 73°; the sample was rocked several degrees at each point to improve the averaging over grains. Fitted positions of 20 low-angle peaks were used in the indexing program *ITO* (Visser, 1969) to obtain monoclinic lattice dimensions of $a = 16.04$, $b = 5.376$, $c = 3.633$ Å, $\beta = 92.87°$, and the space group $P2_1$ was assigned on the basis of systematic absences and molecular volume.

The widths (from fits to pseudo-Voigt line shapes) of peaks which could be unambiguously assigned are plotted as circles in Fig. 1. All of these fits converge to a pseudo-Voigt mixing parameter η in the neighborhood of 0.6, with no obvious trend as a function of width. This fact shows the importance of including both Lorentzian and Gaussian contributions into any general model of anisotropic broadening, as has been done in some (Cox, 1994; Fischer *et al.*, 1995) but not all (Rodríguez-Carvajal, 1997) previous work.

Inspecting the data of Fig. 1, one immediately sees that the (*h*00) and (*hk*0) peaks are quite sharp, whereas peaks with all indices nonzero are the broadest. Particularly noteworthy is the large discrepancy between the widths of the (611) and (800) peaks, which are separated by only 37° in the reciprocal lattice, but fall on the broadest and the narrowest trend lines, respectively, of width *versus* 2θ. Any model of anisotropic broadening based on parameterizing a smooth function of direction within the reciprocal lattice will be hard pressed to account for this observation. On the other hand, the parameters S_{HKL} defined in (3) naturally accommodate the trends in different symmetry directions.

A rather large number of line-shape parameters are required to accurately describe the data set in a Le Bail fit (Le Bail *et al.*, 1988) of the profile. Parameters *U*, *V* and *X* in (6) were set to zero, and *W* and *Y* were set by an extrapolation of the width and shape of the (*h*00) series to $2\theta = 0$. Initial estimates for most of the nine anisotropic broadening parameters were established from the results of individual line-shape fits. For example, the parameter S_{400} is uniquely determined by the width of peaks (*h*00), and once S_{400} and S_{040} have been so fixed, the parameter S_{220} can be derived from the width of (*hk*0) peaks. Ultimately, the nine parameters S_{HKL} appropriate to monoclinic symmetry, along with ζ, *W* and *Y* [equation (6)], were refined in a Le Bail fit to the entire profile. The resulting fit gives a profile *R* factor $R_p = 5.93\%$ and weighted $R_{wp} = 8.22\%$, with $\chi^2 = 7.31$; these values can be compared to $R_p = 10.32\%$, $R_{wp} = 15.47\%$ and $\chi^2 = 26.2$ for the best Le Bail fit with the S_{HKL} all set to zero, and only the conventional Rietveld parameters *U*, *V*, *W*, *X* and *Y* refined. The parameters are given in Table 2, and the

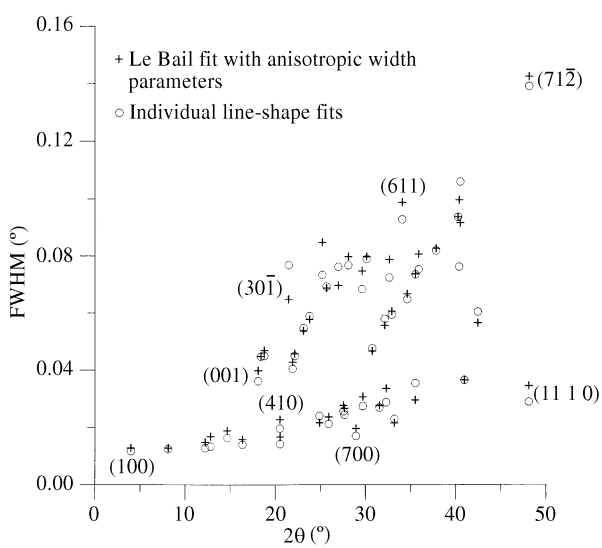

Fig. 1. FWHM *versus* diffraction angle 2θ for sodium *p*-hydroxybenzoate. Plotted are both the widths of pseudo-Voigt fits to individual peaks and the widths in a Le Bail fit of the entire profile, with the line-shape parameters listed in Table 2.

Table 2. *Refined values of anisotropic strain parameters for sodium p-hydroxybenzoate*

The last column shows the Rietveld R_{wp} with the relevant parameter set to zero; for comparison, the best fit with all parameters refined has $R_{wp} = 8.22\%$.

Parameter	Value	R_{wp} (%) when parameter set to zero
S_{400}	$(1.90 \pm 0.05) \times 10^{-11}$	8.63
S_{301}	$(2.8 \pm 0.1) \times 10^{-9}$	8.63
S_{220}	$(1.9 \pm 0.5) \times 10^{-9}$	8.61
S_{202}	$(5.61 \pm 0.06) \times 10^{-8}$	12.95
S_{121}	$(0 \pm 1) \times 10^{-8}$	8.22
S_{103}	$(1.1 \pm 0.1) \times 10^{-8}$	8.23
S_{040}	$(2.2 \pm 0.1) \times 10^{-9}$	8.39
S_{022}	$(8.3 \pm 0.2) \times 10^{-8}$	8.74
S_{004}	$(1.25 \pm 0.01) \times 10^{-7}$	10.5
ζ	0.404 ± 0.005	10.81

widths from this refinement are plotted, for comparison with the measured widths, in Fig. 1.

The measured and fitted widths are also compared in Fig. 2, which does not show the evolution of individual families in certain directions as clearly as Fig. 1, but does give a very encouraging indication of the agreement between model and experimental results. A portion of the Le Bail fit is shown in Fig. 3, again demonstrating excellent agreement between the experimental data and the model presented in §2.

It is natural to ask whether all nine of the symmetry-allowed anisotropic strain parameters are actually needed to obtain an acceptable fit to the line shape. This question is addressed by fits with each in turn of the nine allowed parameters S_{HKL}, as well as the Lorentzian mixing parameter ζ, set to zero. In each case, all of the other parameters were adjusted for the best least-squares fit; the resulting values of R_{wp} are listed in Table 2. The results indicate that seven of the nine anisotropic strain parameters have a significant role in producing an acceptable line-shape fit, and that it is important to include Lorentzian contributions to the anisotropic line shape. It is likely that the relative unimportance of S_{121} and S_{103} represent details of the present sample rather than a universal property of the model developed here. One can also see that the S_{HKL} parameters really act independently by looking at the correlation matrix in the least-squares refinement. If any of the parameters were redundant, they would show elements near unity. In fact, the two largest correlations were 58%, between S_{301} and S_{202}, and 54%, between S_{022} and S_{004}. This implies that each parameter has an independent influence on the model.

It is not easy to visualize the form of $\Gamma_A(hkl)$ from equations (3) and (4). Indeed, it is not immediately clear whether this is a smooth function of the direction $\hat{Q}$ of the *hkl* reflection in reciprocal space, since it is defined only on the reciprocal lattice. Because Γ_A increases in proportion to the diffraction order, it is sensible to consider the scaled width, $\Gamma_A / \tan\theta$. Fig. 4 depicts three sections of $\Gamma_A(\hat{Q})/\tan\theta$ for the reflection list and S_{hkl} parameters of the present refinement, which show that the scaled width is a smooth function of direction in reciprocal space, and also that the refined pattern of widths is quite different from an ellipsoid in reciprocal space.

3.2. Rb_3C_{60}

Anisotropic broadening of powder diffraction peaks in the alkali fulleride superconductor Rb_3C_{60} was first noted by Zhu *et al.* (1991). Cox (1994) had developed a model of the anisotropic variation of line widths which has a significant effect on the quality of fits attainable, and which allows the conclusion that the material is actually non-stoichometric, with a few percent cation vacancies (Fischer *et al.*, 1995; Bendele *et al.*, 1998). His

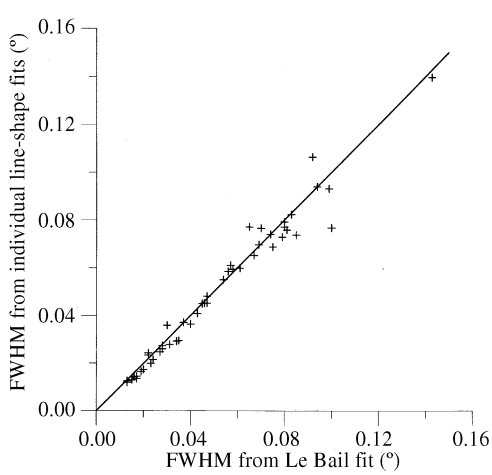

Fig. 2. Comparison of FWHM from the Le Bail fit to individual peak fits, for the same data shown in Fig. 1.

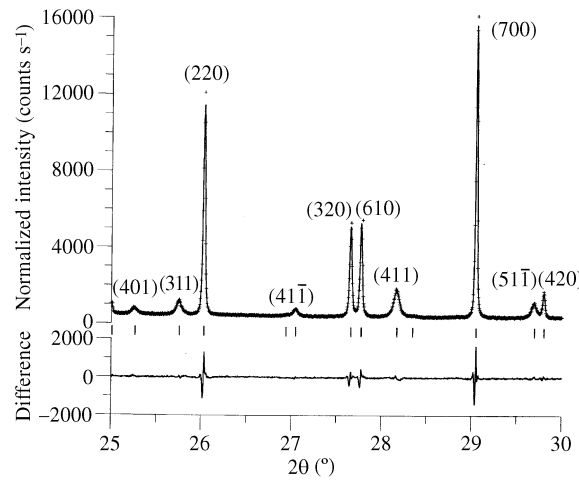

Fig. 3. Part of the Le Bail fit to the diffraction profile of sodium *p*-hydroxybenzoate.

approach is to multiply the width from the Thompson–Cox–Hastings line-shape model [parameters U, V, W, X and Y in (5)] by a function of the direction of the Bragg peak in reciprocal space, $g(\hat{Q})$, and to parameterize that function through symmetry-adapted spherical harmonics. In this section, we compare the results of that approach with the present method, using an Rb_3C_{60} data set that has been discussed in previous work (Fischer *et al.*, 1995).

The Rb_3C_{60} sample was prepared by vapor transport in a sealed capillary, and measured on beamline X3B1 of the National Synchrotron Light Source with a double-crystal Si(111) monochromator and Ge(111) analyzer at an X-ray wavelength of $\lambda = 1.14964$ Å. The sample has a lattice parameter of 14.431 Å. The widths of peaks which are fully resolved in the powder diffraction pattern are plotted in Fig. 5, from which it can be seen that peaks in the (100) direction are approximately twice as broad as those along (111). The inset to Fig. 5 shows a limited range of the data, encompassing the (311) and (222) peaks, with widths in the ratio of 1.7 : 1. A Le Bail fit to the entire spectrum (5–66°) without anisotropic broadening gives $R_{wp} = 9.1\%$ ($\chi^2 = 7.02$).

For the case of cubic symmetry, the Cartesian coordinates of $g(\hat{Q})$ are (h', k', l'), with $h' = h(h^2 + k^2 + l^2)^{-1/2}$, *etc.* $g(h', k', l')$ is expanded as a series,

$$g(h', k', l') = 1 + C_4K_4 + C_6K_6 + \cdots$$

with

$$K_4(h', k', l') = 5(h'^4 + k'^4 + l'^4)/2 - 3/2$$

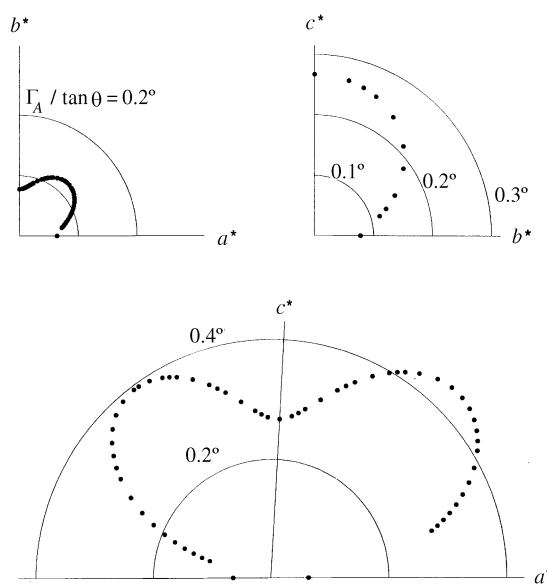

Fig. 4. Reduced anisotropic width ($\Gamma_A/\tan\theta$) for three sections through the reciprocal space of monoclinic sodium *p*-hydroxybenzoate.

etc. [Higher terms in the series have been given by Järvinen *et al.* (1970).] A Le Bail fit gives a weighted $R_{wp} = 3.42\%$ ($\chi^2 = 2.15$) with the anisotropic width parameters $\{C_j\}$ listed in Table 3.

Within the present model for strain broadening in a cubic system, there are only two independent parameters, S_{400} and S_{220}. As for the case of sodium *p*-hydroxybenzoate discussed above, the strain-dependent parameters appearing in the Voigt-adapted Rietveld formalism, U, V and X, were set to zero. It was found that the parameters W and Y, which give the size contribution (broadening of low-angle peaks), converged to values which were essentially zero, and so they were left out of the final refinement. The Le Bail fit converges to the parameters listed in Table 3, with $R_{wp} = 3.45\%$, $\chi^2 = 2.19$. There is no significant difference between line-shape fits with the spherical harmonic model (with nine adjustable line-shape parameters) and the present work (with three). Clearly, this model condenses the necessary flexibility into fewer parameters than the spherical harmonic approximation, at least for this particular example. It is tempting to suggest that this is due to the validity of the underlying physical model, a point which is discussed below.

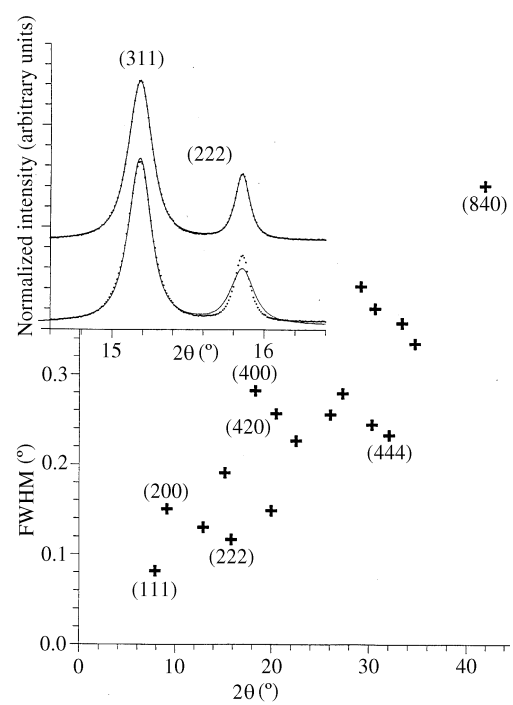

Fig. 5. Diffraction peak width *versus* diffraction angle for the peaks which can be resolved and indexed unambiguously from a powder pattern of f.c.c. Rb_3C_{60}. The inset at the top shows a limited range of the data, fitted by a model with two different peak widths (upper trace) and with the widths constrained to be equal (lower trace). Reprinted from *J. Phys. Chem. Solids* (1995), **56**, 1445–1457, with permission from Elsevier Science.

Table 3. *Comparison of parameters for line-shape fits of cubic Rb_3C_{60}*

Comparison is for fits according to Cox's (1994) spherical harmonic expansion and the model described in the present work. In each case, besides those listed, four other parameters were refined: lattice parameter, zero-shift, low-angle peak-asymmetry parameter and background normalization.

Spherical harmonic expansion	Present work
$U = 1.2166$	$U = V = W = X = Y = 0$
$V = -0.3915$	
$W = 0.0222$	
$X = 0.823$	
$Y = 0.0054$	
$C_4 = 0.418$	$S_{400} = S_{040} = S_{004} = 3.43 \times 10^{-8}$
$C_6 = -0.0328$	$S_{220} = S_{202} = S_{022} = -1.13 \times 10^{-8}$
$C_8 = -0.0574$	$\zeta = 0.558$
$C_{10} = -0.0057$	
$R_{wp} = 3.42\%$	$R_{wp} = 3.45\%$
$\chi^2 = 2.15$	$\chi^2 = 2.19$

4. Comparison with other work

The present idea of anisotropic broadening through correlations of metric parameters was initially described by two other groups. The first work was by Thompson, Reilly & Hastings (1987), specifically for the case of hexagonal La_5Ni, in which a large lattice strain was introduced by loading and removing interstitial hydrogen. While their basic principle was along the lines described here, their expression for the line width was not compatible with hexagonal symmetry, in the sense that reflections (h, k, l), $(-k, h + k, l)$ *etc*. do not have the same width. They obtained satisfactory results, presumably because the reflection list used in their refinement was sorted into a particular order, *e.g.* $h \geq k \geq 0$ and $l \geq 0$. Nevertheless, we cannot regard their formulation as generally applicable.

The other previous formulation of this model was outlined for tetragonal La_2NiO_4 by Rodríguez-Carvajal *et al*. (1991), and made publicly available in the program *FULLPROF* (Rodríguez-Carvajal, 1997). In that program, the anisotropic broadening line shape is restricted to a Gaussian form; as we have seen (Table 2), this can produce a serious degradation of the quality of line-shape fit obtainable. More seriously, not all of the parameters (fifteen for triclinic, nine for monoclinic, *etc*.) are available. [There are minor notational differences in that the *FULLPROF* treatment uses the standard deviation and correlation parameters $\sigma_i = C_{ii}^{1/2}$ and $C_{ij}/(\sigma_i\sigma_j)$. Also, for anisotropic strain broadening in the monoclinic system, *FULLPROF* takes c as the twofold axis, but the results are here translated to the b setting for comparison with the present work.] For monoclinic symmetry, *FULLPROF* treats the two parameters C_{13} and C_{55} as separately refinable, although they both appear in the term of (3) proportional to h^2l^2 and therefore have identical actions on the widths of powder peaks. Furthermore, correlations between metric parameters A and E and between C and E are neglected, so that parameters S_{301} and S_{103} do not appear. Another shortcoming of the treatment in *FULLPROF* is that it is not able to handle cubic systems [equation (8)]. However, it is worth noting that the *FULLPROF* treatment does agree with the present work on the parameters required and available for tetragonal, orthorhombic and hexagonal systems.

Popa (1998) has presented a mathematical treatment of strain broadening which is essentially identical to the present work, with two important differences. He assumes that the strain broadening affects only the Gaussian component of a Voigt lineshape; as discussed above, the strain broadening in real samples contains a Lorentzian component which is crucial for obtaining a useful fit, even though mathematical difficulties arise in justifying it. Furthermore, Popa's treatment is more general, as it applies only the Laue symmetry instead of degeneracy in the powder pattern in considering symmetry restrictions. For example, in tetragonal crystals with $4/m$ Laue symmetry, reflections hkl and khl are not equivalent even though they overlap in a powder pattern. Popa's treatment (translated into the present notation) allows such peaks to have different width, by including a term $S_{310}(h^3k - hk^3)$. The trigonal Laue group $\overline{3}$ presents another example, with (hexagonal) reflections (h, k, l) and $(h + k, \overline{k}, l)$ constrained to equal widths in the present work, but distinguishable in Popa's model. Clearly, a Le Bail fit (without structural information) will be unstable if it refines parameters which control the widths of peaks which have the same position in a powder pattern, and so the present formalism should be used in such a case. However, if a structural model is known which distinguishes powder-degenerate peaks by their intensity, it may be useful to separately refine their widths as described by Popa.

5. Discussion

The present approach has been termed phenomenological because it relates a microscopic explanation for lattice strains to the observed diffraction profiles, even though it cannot predict the actual values of the strain parameters. It is of interest to compare this with a model of anisotropic strain broadening in cubic crystals by Stokes & Wilson (1944). They assumed that a sample of cold-worked metal was characterized by a random but isotropic distribution of stress, so that the sample strain might vary as a function of direction due to the anisotropy of the elasticity. On these very general grounds, they predicted that the width of each reflection should be given by

$$\Gamma = \left[A + B\frac{h^2k^2 + k^2l^2 + h^2l^2}{(h^2 + k^2 + l^2)^2}\right]^{1/2} \tan\theta \qquad (7)$$

where A and B depend only on the elastic constants and the mean-square stresses of the sample. Within the present model, cubic systems are characterized by two independent strain parameters, S_{400} and S_{220}, so that the anisotropic contribution to the line width is

$$\begin{aligned}\Gamma_{2\theta}(hkl) &= \frac{[S_{400}(h^4+k^4+l^4)+S_{220}(h^2k^2+k^2l^2+h^2l^2)]^{1/2}}{(h^2+k^2+l^2)/a_0^2} \times \tan\theta \\ &= \left[S_{400}+(S_{220}-2S_{400})\frac{h^2k^2+k^2l^2+h^2l^2}{(h^2+k^2+l^2)^2}\right]^{1/2} \times \tan\theta a_0^2\end{aligned} \tag{8}$$

where a_0 is the cubic lattice parameter. It is immediately seen that these expressions are identical, differing only in the definitions of their phenomenological parameters.

Micro-strain in a powder sample may originate from a distribution of dislocations within the individual grains. The fundamental approach would be to work out the elastic field of a particular type of defect, to calculate the diffraction line shape for each reflection (hkl), and then perform a suitable average over orientations. This program is forbiddingly complicated for any but the simplest materials; it has been carried out for hexagonal-close-packed (h.c.p.) (Klimanek & Kuzel, 1989) and face-centred-cubic (f.c.c.) (Ungár & Borbély, 1996) metals. In both cases, the influence of a particular defect on a particular reflection is governed by a contrast factor $\bar{C}$, which can be evaluated (with considerable effort) from elasticity theory (Groma *et al.*, 1988). Ungár & Borbély (1996) measured the widths of six powder peaks in a cold-worked sample of copper powder. Their data of width *versus* diffraction angle look very similar to the first six points in Fig. 5. They found that the introduction of the contrast factor $\bar{C}$ into the abscissa of a modified Williamson–Hall plot gave perfect agreement with their data. Indeed, their tabulated contrast factor is linear in the combination of Miller indices which arises in this work; in particular, it is given (within one part in 10^4) by

$$\bar{C} = 0.3040 - 0.6141\frac{h^2k^2+k^2l^2+h^2l^2}{(h^2+k^2+l^2)^2}. \tag{9}$$

More recently, motivated by the present work, Ungár & Tichy (1999) have shown that the contrast factor generated by any type of dislocation in a cubic material must have this dependence on the Miller indices.

In summary, this paper has presented a technique for handling anisotropic strain broadening in powder diffraction patterns which is based on a reasonable physical assumption and which provides a very good match to the data for the two examples given. Furthermore, in the case of cubic systems, it makes contact with the results of a microscopic treatment. In future work, it will be important to determine whether this method is universally applicable, and whether its premises can be derived with greater rigor from the physics of micro-strain.

APPENDIX *A*

Since the original submission of this manuscript, the present formulation of anisotropic strain broadening has been adapted into the widely-used *GSAS* package (Larson & Von Dreele, 1994). Some of the parameters have been redefined to integrate smoothly into the *GSAS* code, and so a summary of the differences between notation used in *GSAS* and the present work is given here for the convenience of users.

(1) The scale of the parameters S_{hkl} is defined to give them numerical values closer to unity, by defining the anisotropic strain as $\delta d/d = \pi[\sigma^2(M_{hkl})]^{1/2}/(18000M_{hkl})$. For fixed wavelength experiments, this leads to an angular width in 2θ equal to $(360^\circ/\pi)(\delta d/d)\tan\theta$.

(2) *GSAS* treats $\delta d/d$ as the variance of a Gaussian lineshape, but the half-width at half-maximum of a Lorentzian. This produces small numerical differences in the fitting parameters, but is of no significance in the quality of the fit.

(3) The number of different covariance matrix elements C_{ij} contributing to each S_{HKL} is included explicitly, so that equation (3) becomes

$$\begin{aligned}\sigma^2(M_{hkl}) = {} & S_{400}h^4 + S_{040}k^4 + S_{004}l^4 + 3(S_{220}h^2k^2 \\ & + S_{202}h^2l^2 + S_{022}k^2l^2) + 2(S_{310}h^3k + S_{103}hl^3 \\ & + S_{031}k^3l + S_{130}hk^3 + S_{301}h^3l + S_{013}kl^3) \\ & + 3(S_{211}h^2kl + S_{121}hk^2l + S_{112}hkl^2).\end{aligned}$$

I have profited in many ways from useful discussions with David Cox. I am also grateful to G. M. Bendele, R. E. Dinnebier, J. E. Fischer, M. Pink and J. Sieler for contributions to the data collection and analysis. R. E. Dinnebier, J. I. Langford, A. Le Bail, R. Von Dreele, and an anonymous referee have made useful suggestions about this presentation. This work has been partially supported by the National Science Foundation grant No. DMR95-01325. The SUNY X3 beamline at the National Synchrotron Light Source is supported by the Division of Basic Energy Sciences of the US Department of Energy (DE-FG02-86ER-45231). Research was carried out at the National Synchrotron Light Source at Brookhaven National Laboratory, which is supported by the US Department of Energy, Division of Materials Sciences and Division of Chemical Sciences.

References

Bendele, G. M., Stephens, P. W. & Fischer, J. E. (1998). *Europhys. Lett.* **41**, 553–558.

Caglioti, G., Paoletti, A. & Ricci, F. P. (1958). *Nucl. Instrum. Methods*, **3**, 223–228.
Cox, D. E. (1994). Personal communication.
David, W. I. F. & Jorgensen, J. D. (1995). *The Rietveld Method*, edited by R. A. Young, pp. 197–226. Oxford University Press.
Dinnebier, R. E., Stephens, P. W., Pink, M. & Sieler, J. (1995). Abstract in *National Synchrotron Light Source Activity Report for 1995*, Publication BNL 52496, p. B47. Upton: Brookhaven National Laboratory.
Fischer, J. E., Bendele, G., Dinnebier, R., Stephens, P. W., Lin, C. L., Bykovetz, N. & Zhu, Q. (1995). *J. Phys. Chem. Solids*, **56**, 1445–1457.
Groma, I., Ungár, T. & Wilkens, M. (1988). *J. Appl. Cryst.* **21**, 47–53.
Järvinen, M., Merisalo, M., Pesonen, A. & Inkinen, O. (1970). *J. Appl. Cryst.* **3**, 313–318.
Klimanek, P. & Kuzel, R. Jr (1989). *J. Appl. Cryst.* **22**, 299–307.
Larson, A. C. & Von Dreele, R. B. (1994). *GSAS – General Structure Analysis System*. Los Alamos National Laboratory Report LAUR 86-748. Available electronically by anonymous ftp from ftp.mist.lansce.lanl.gov.
Le Bail, A. (1992). *Accuracy in Powder Diffraction II: Proceedings of the International Conference May 26–29*, edited by E. Prince & J. K. Stalick, NIST Special Publication, Vol. 846, pp. 142–153. Washington, DC: US Government Printing Office.
Le Bail, A., Duroy, H. & Fourquet, J. L. (1988). *Mater. Res. Bull.* **23**, 447–452.
Le Bail, A. & Jouanneaux, A. (1997). *J. Appl. Cryst.* **30**, 265–271.
Mendenhall, W., Schaeffer, R. L. & Wackerly, D. D. (1986). *Mathematical Statistics with Applications*. Boston: Duxbury Press.
Popa, N. C. (1998). *J. Appl. Cryst.* **31**, 176–180.
Rietveld, H. M. (1969). *J. Appl. Cryst.* **2**, 65–71.
Rodríguez-Carvajal, J. (1997). *Short Reference Guide of the Program FULLPROF*. Available electronically by anonymous ftp in the directory pub/divers/fullp on the computer bali.saclay.cea.fr.
Rodríguez-Carvajal, J., Fernández-Díaz, M. T. & Martínez, J. L. (1991). *J. Phys. Condens. Matter*, **3**, 3215–3234.
Stokes, A. R. & Wilson, A. J. C. (1944). *Proc. Phys. Soc. London*, **56**, 174–181.
Thompson, P., Cox, D. E. & Hastings, J. B. (1987). *J. Appl. Cryst.* **20**, 79–83.
Thompson, P., Reilly, J. J. & Hastings, J. B. (1987). *J. Less Common Met.* **129**, 105–114.
Ungár, T. & Borbély, A. (1996). *Appl. Phys. Lett.* **69**, 3173–3175.
Ungár, T. & Tichy, G. (1999). *Phys. Status Solidi*. Submitted.
Visser, J. W. (1969). *J. Appl. Cryst.* **2**, 89–95.
Von Dreele, R. B. & Line, C. M. B. (1997). *Abstracts of the Fifth European Powder Diffraction Conference*, Parma, edited by G. Artioli, A. Gualtieri & M. Zanni, p. 53.
Zhu, Q., Zhou, O., Coustel, N., Vaughan, G. B. M., McCauley, J. P. Jr, Romanow, W. J., Fischer, J. E. & Smith, A. B. III (1991). *Science*, **254**, 545–548.